

5. A. S. Kadinova and V. I. Krivizhenko, "Cooling capacities of nozzles of different constructions," *Metalloved. Term. Obrab. Met.*, No. 3, 26 (1968).
6. A. S. Kadinova and G. N. Kheifets, "Factors affecting heat exchange in water-jet cooling," *Metalloved. Term. Obrab. Met.*, No. 1, 10 (1974).
7. M. Kumada and I. Mabuchi, "Studies on the heat transfer of impinging jet. I. Mass transfer for two-dimensional jet of air, impinging normally on a flat plate," *Bull. Jpn. Soc. Mech. Eng.*, 13, No. 55, 77 (1970).
8. D. C. McMurray, P. S. Myers, and O. A. Uehara, "Influence of impinging jet variables on local heat transfer coefficients along a flat surface with constant heat flux," *Proceedings of the Third International Heat Transfer Conference, Chicago, Vol. 2 (1966)*, p. 292.
9. S. Sitharamayya and K. S. Raju, "Heat transfer between an axisymmetrical jet and a plate held normal to the flow," *Can. J. Chem. Eng.*, 47, 365 (1969).
10. Y. Yin-Chao, "Heat transfer characteristics of a bubble-induced water jet, impinging on an ice surface," *Int. J. Heat Mass Transfer*, 18, Nos. 7/8, 917 (1975).

#### HEAT-TRANSFER MECHANISM AT A GAS-FIBER BOUNDARY

I. G. Chumak and V. G. Pogontsev

UDC 536.244:621.186.4

Heat conduction in a fibrous dispersed material with a gas filler is studied.

Molecular thermal conductivity of a gas in a free volume, introduced by the molecular-kinetic theory, results from intermolecular interactions in the gas.

In dispersed two-component materials there are not only intermolecular interactions but also interactions of gas molecules with the solid component. The heat-transfer mechanism by gas molecules in a dispersed material is studied together with the interaction at the boundary between the gas and the solid component, and the corresponding molecular thermal conductivity of the gas  $\lambda_m$  is determined, e.g., from the relation [1]

$$\lambda_m = \lambda_g [1 + B/(H\delta)]^{-1}, \quad (1)$$

where B is a constant for a given gas and H is the pressure of the gas.

The simultaneous study of intermolecular interactions and interactions at the gas-solid boundary in a dispersed material complicates the study of the separate mechanisms. At the same time, knowledge of the physics of the heat-transfer process in a boundary layer whose thickness is comparable with the mean free path of gas molecules enables us to study the heat-transfer mechanism in dispersed materials more completely, to discover the physical nature of the transport coefficients, and to establish their qualitative behavior and numerical values.

Since heat transfer between a gas and a solid takes place in a layer of thickness  $\bar{l}^*$ , it is expedient to study heat transfer by the thermal conductivity of a gas filler in a dispersed material by taking separate account of intermolecular interactions and interactions of gas molecules with the solid. Therefore, we use a model with interpenetrating components [1] to represent fibrous materials with a random structure, and introduce a supplementary thermal resistance of a layer of thickness  $\bar{l}^*$  at the gas-fiber boundary. Figure 1a shows one-eighth of the elementary cell under study, and Fig. 1b the circuit diagram of the thermal resistances.

Figure 1b illustrates the physical meaning of the proposed method for taking separate account of intermolecular interactions and interactions at a gas-fiber boundary. Suppose there are N gas molecules in an elementary cell. Since air at atmospheric pressure is a rarefied gas in which binary molecular interactions predominate, at any arbitrary instant a

---

Odessa Technological Institute of the Refrigeration Industry. Translated from *Inzhenerno-Fizicheskii Zhurnal*, Vol. 36, No. 1, pp. 55-61, January, 1979. Original article submitted January 2, 1978.

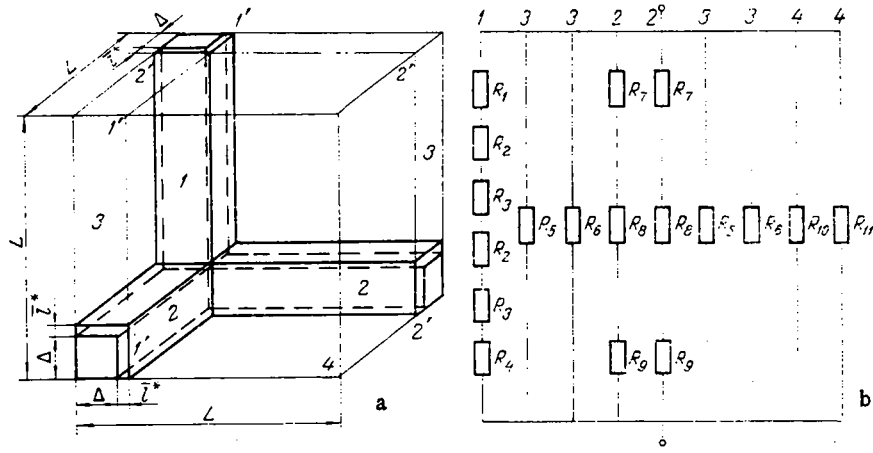


Fig. 1. Scheme for calculating the effective thermal conductivity of a system with interpenetrating components: a) one-eighth of a cell; b) circuit diagram of thermal resistances.

portion  $N_2$  of the molecules will be interacting with one another, and a portion  $N_1$  with the fiber. The result of the first type of interactions is the transfer of thermal energy by the thermal conductivity of the gas, and the result of the second type of interaction is heat transfer at the gas-fiber boundary. Since the two types of interaction occur simultaneously and independently of one another, the diagram presented here shows the resistances  $R_5$  and  $R_6$  connected in parallel with the resistances  $R_7$ ,  $R_8$ , and  $R_9$ . All series connections of resistances represent taking account of interactions of molecules of the boundary layer of the gas with a fiber.

We choose the adiabatic planes 1'-1' and 2'-2' parallel to the common direction of heat flow and the lateral faces of the cell at the separate sections 1, 2, 3, 4. We express the thermal resistances of the parts of an elementary cell  $R_i$  by the equations for a flat wall

$$\begin{aligned}
 R_1 &= \frac{L}{\lambda_1 \Delta^2}; & R_2 &= \frac{\Delta}{\lambda_1 \bar{l}^* \Delta}; & R_3 &= \frac{1}{\alpha \bar{l}^* \Delta}; & R_4 &= \frac{1}{\alpha \bar{l}^{*2}}; \\
 R_5 &= \frac{[L - (\bar{l}^* + \Delta)]}{\lambda_g^* [L - (\bar{l}^* + \Delta)] (\bar{l}^* + \Delta)}; & R_6 &= \frac{[L - (\bar{l}^* + \Delta)]}{\lambda_r [L - (\bar{l}^* + \Delta)] (\bar{l}^* + \Delta)}; \\
 R_7 &= \frac{\Delta}{\lambda_1 [L - (\bar{l}^* + \Delta)] \Delta}; & R_8 &= \frac{1}{\alpha [L - (\bar{l}^* + \Delta)] (\bar{l}^* + \Delta)}; \\
 R_9 &= \frac{1}{\alpha [L - (\bar{l}^* + \Delta)] \bar{l}^*}; & R_{10} &= \frac{L}{\lambda_g^* [L - (\bar{l}^* + \Delta)]^2}; \\
 R_{11} &= \frac{L}{\lambda_r [L - (\bar{l}^* + \Delta)]^2}.
 \end{aligned} \tag{2}$$

We write the total or effective thermal resistance  $R$  of an elementary cell in the form

$$\frac{1}{R} = \frac{1}{R_1 + 2R_2 + 2R_3 + R_4} + \frac{2}{R_5} + \frac{2}{R_6} + \frac{2}{R_7 + R_8 + R_9} + \frac{1}{R_{10}} + \frac{1}{R_{11}}. \tag{3}$$

The total thermal resistance of this volume filled with a homogeneous material with an effective thermal conductivity  $\lambda_{\text{eff}}$  is

$$R = \frac{1}{\lambda_{\text{eff}} L}. \tag{4}$$

Equating (3) and (4), taking account of (2), and making some algebraic transformations, we obtain an expression for the effective thermal conductivity of a structure with interpenetrating components

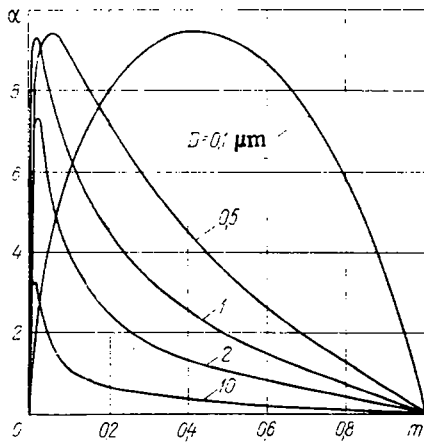


Fig. 2. Heat-transfer coefficient  $\alpha$ ,  $10^4$  W/m<sup>2</sup>·deg K, at a gas-fiber boundary as a function of porosity.

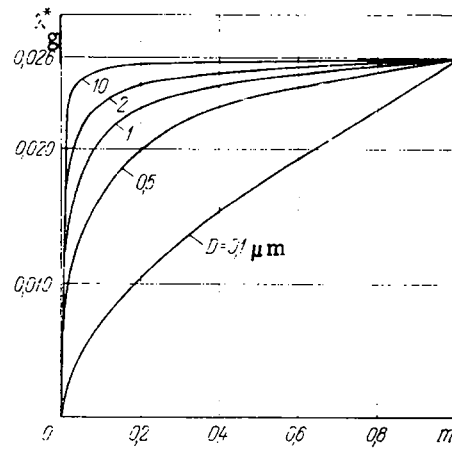


Fig. 3. Thermal conductivity  $\lambda_g^*$ , W/m·deg K, of a gas inside a dispersed fibrous material as a function of porosity.

$$\lambda_{\text{eff}} = \lambda_1 \left\{ \nu [1 + (C + S)^2] + \frac{C^2 S}{(S + 2C^2) - \beta(C^2 + 2SC)} + \frac{2[1 - (C + S)]}{1 + \beta \left(1 + \frac{S}{C - S}\right)} \right\}, \quad (5)$$

where

$$\nu = \frac{\lambda_g^* + \lambda_r}{\lambda_1}; \quad \beta = \frac{\lambda_1}{\alpha l^*}; \quad S = \frac{\bar{l}^*}{L} = \frac{4\bar{l}^* C}{D\sqrt{\pi}}, \quad (6)$$

and the parameter C is related to the porosity m by the expression [1]

$$m = 2C^3 - 3C^2 + 1. \quad (7)$$

We write the parameter S in another form by using the expression for the average distance between fibers  $\bar{\delta}$  in an elementary cell [1]:

$$\bar{\delta} = D.C. \quad (8)$$

Then

$$S = \frac{4}{\sqrt{\pi}} Kn^*, \quad Kn^* = \frac{\bar{l}^*}{\bar{\delta}}. \quad (9)$$

In accord with the method assumed above of taking separate account of intermolecular interactions and interactions at a gas-solid boundary, we obtain relations for the heat-transfer coefficient at a gas-fiber boundary and the molecular thermal conductivity of a gas inside a fibrous dispersed material.

As shown in [3], the number of collisions  $\nu_1$  of a molecule with the surfaces of fibers is

$$\nu_1 = \bar{\nu} F_{sp} / 4m, \quad (10)$$

where  $F_{sp} = F_{s0}/V$ . The volume  $V_1$  occupied by the gas at a distance  $\bar{l}^*$  from a fiber within the limits of an elementary cell (Fig. 1) is

$$V_1 = 2\Delta^3 + 3L\bar{l}^*(\bar{l}^* + 2\Delta) - 2(\bar{l}^* + \Delta)^3. \quad (11)$$

The total number of molecules in the volume  $V_1$  under normal conditions is

$$N_1 = n_0 V_1. \quad (12)$$

The total number of collisions of gas molecules in a layer of thickness  $\bar{l}^*$  with the surfaces of fibers is

$$\nu_0 = \nu_1 N_1. \quad (13)$$

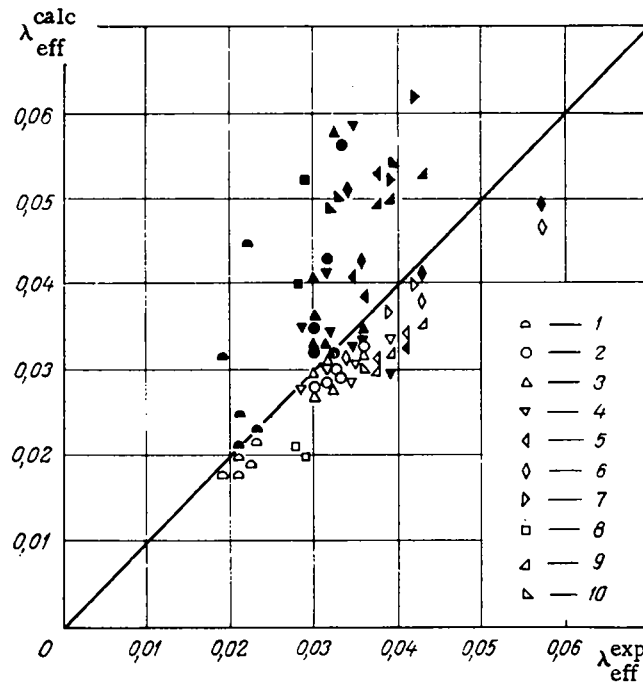


Fig. 4. Comparison of calculated and experimental values of the effective thermal conductivity of fibrous materials: 1) fiberglass AA, fiber diameter 1.015  $\mu\text{m}$ , average temperature 192°K [5]; 2) AAAA, 0.56  $\mu\text{m}$ , 297°K [4]; 3) AA, 1.14  $\mu\text{m}$ , 297°K [4]; 4) fiberglass B, 3.43  $\mu\text{m}$ , 297°K [4]; 5) fiberglass PF-600, 12.2  $\mu\text{m}$ , 297°K [4]; 6) fiberglass A, 2.58  $\mu\text{m}$ , 338°K [6]; 7) fiberglass B, 1.51  $\mu\text{m}$ , 422°K [6]; 8) rock wool, 10.0  $\mu\text{m}$ , 190°K [2]; 9) fiberglass, 15.2  $\mu\text{m}$ , 297, 311, 338°K [7]; 10) fiberglass, 0.685  $\mu\text{m}$ , 297, 311, 338°K [7]. Open points calculated by Eq. (5); solid points calculated by (28).  $\lambda$  is in W/m·deg K.

As a result of  $v_0$  collisions of gas molecules in a layer of thickness  $\bar{l}^*$  an amount of energy

$$\Delta E = \frac{3}{2} ak(T_i - T_s)v_0, \quad (14)$$

is transferred to fiber surfaces, where  $T_i - T_s$  is the temperature difference across the layer of gas at a distance  $\bar{l}^*$  from a fiber.

Substituting Eqs. (10)-(13) into (14) and making some transformations, we obtain

$$\Delta E = \frac{3}{8} akn_0\bar{v} \left[ \frac{2C^3 - 3(S^2 - 2SC) - 2(C - S)^3}{m} \right] F_{so} (T_i - T_s). \quad (15)$$

Taking account of the Eucken correction for a polyatomic gas, we finally obtain

$$\Delta E = \alpha F_{so} (T_i - T_s), \quad (16)$$

where

$$\alpha = \frac{3}{32} akn_0\bar{v} \left( \frac{\gamma - 1}{\gamma - 1} \right) \left[ \frac{2C^3 - 3(S^2 - 2SC) - 2(C - S)^3}{m} \right]. \quad (17)$$

Figure 2 shows the dependence of the heat-transfer coefficient at a gas-fiber boundary on porosity for various fiber diameters, atmospheric air pressure, average temperature 300°K, and accommodation coefficient  $\alpha = 1$ .

We obtain an expression for the molecular thermal conductivity of a gas inside a dispersed material resulting from intermolecular interactions in the following way.

According to the molecular-kinetic theory, the molecular thermal conductivity of a gas in a free volume is given by the expression

$$\lambda_g = \frac{C_p \rho_g \bar{v}}{3M} \bar{l} = k_0 \bar{l}, \quad (18)$$

where  $k_0$  is a quantity depending on the pressure, temperature, and kind of gas.

A similar expression can be written for a gas inside a dispersed material:

$$\lambda_g^* = k_0 \bar{l}^*. \quad (19)$$

Kostylev [3] showed that  $\bar{l}^*$  is always less than  $\bar{l}$ :

$$\bar{l}^* = \left[ \frac{1}{\bar{l}} + \frac{F_{sp}}{4m} \right]^{-1}. \quad (20)$$

We obtain an expression for  $F_{sp}$  from the model shown in Fig. 1. The total fiber surface in an elementary cell is

$$F_{so} = 6\Delta(L - \Delta) \quad (21)$$

for an elementary cell whose volume is

$$V = L^3. \quad (22)$$

According to [1]

$$\Delta = D \sqrt{\pi}/4, \quad L = \Delta/C. \quad (23)$$

Then

$$F_{sp} = \frac{F_{so}}{V} = \frac{24C^2(1-C)}{D \sqrt{\pi}}. \quad (24)$$

Substituting (24), (20), and (18) into (19) and making some algebraic transformations, we obtain

$$\lambda_g^* = \lambda_g \left[ 1 + \frac{\bar{l}}{D} \cdot \frac{6C^2(1-C)}{m \sqrt{\pi}} \right]^{-1}. \quad (25)$$

Using (8) we transform Eq. (25) to the form

$$\lambda_g^* = \lambda_g (1 + b Kn)^{-1}, \quad (26)$$

where

$$b = 6C(1-C)/m \sqrt{\pi}, \quad (27)$$

and  $0 \leq b \leq \infty$  (the value  $b = \infty$  is obtained by evaluating the indeterminate form  $0/0$ ).

Figure 3 shows the dependence of the molecular thermal conductivity of a gas inside a dispersed fibrous material on the porosity calculated by Eq. (25) for various values of the fiber diameter at atmospheric air pressure and an average temperature of 300°K.

Analysis of Eqs. (17) and (25) shows that as a fibrous dispersed material is compacted  $\bar{l}^*$  is decreased proportionally, the number of collisions of gas molecules with fibers increases, and the number of intermolecular interactions decreases. This leads to an improvement in heat transfer in the boundary layer and a decrease in the molecular thermal conductivity of the gas  $\lambda_g^*$ . For a porosity corresponding to the maximum value of  $\alpha$  the number of molecules  $N$  in the volume of the dispersed material is sharply decreased, heat transfer between gas and fiber is worsened, and at  $m = 0$ ,  $\alpha = 0$ . For an increase in fiber diameter (all other conditions remaining the same) the average distance between fibers and the number of intermolecular interactions increase. As a result  $\lambda_g^*$  increases and  $\alpha$  decreases.

Figure 4 compares experimental values of the effective thermal conductivity for various fibrous materials with corresponding values calculated by the relation [1]

$$\lambda_{eff} = \lambda_1 \left[ C^2 + v(1-C)^2 + \frac{2vC(1-C)}{vC + (1-C)} \right] \quad (28)$$

and by (5). It is clear from Fig. 4 that the values calculated by (5), which takes account of heat transfer at the gas-fiber boundary, are in better agreement with experiment than values calculated by (28).

#### NOTATION

$\lambda_g^*$ ,  $\lambda_g$ , molecular thermal conductivity of gas inside a dispersed material and in a free volume; Kn, Knudsen number;  $\bar{l}$ ,  $\bar{l}^*$ , mean free path of gas molecules in a free volume and inside a dispersed material;  $\lambda_f$ , thermal conductivity of fiber;  $\lambda_r$ , radiative heat-transfer coefficient;  $\alpha$ , heat-transfer coefficient of gas-fiber boundary in a layer of thickness  $\bar{l}^*$ ;  $\lambda_{eff}$ , effective thermal conductivity of dispersed material; D, fiber diameter;  $\Delta$ , L, elementary cell parameters;  $C_p$ ,  $\rho_g$ , specific heat and density of gas filler, respectively;  $\bar{v}$ , average velocity of thermal motion of gas molecules; M, molecular weight of gas;  $F_{sp}$ , specific surface of solid phase per unit volume of dispersed material; m, porosity; k, Boltzmann constant,  $1.38 \cdot 10^{-23}$  J/deg;  $n_0$ , Loschmidt number,  $2.69 \cdot 10^{25}$  m<sup>-3</sup>;  $T_1$ , temperature of gas at a distance  $\bar{l}^*$  from fiber surface;  $T_s$ , temperature of fiber surface;  $\alpha$ , accommodation coefficient;  $\gamma$ , ratio of specific heat of gas at constant pressure to specific heat at constant volume.

#### LITERATURE CITED

1. G. N. Dul'nev and Yu. P. Zarichnyak, Thermal Conductivity of Mixtures and Composite Materials [in Russian], Énergiya, Leningrad (1974).
2. M. G. Kaganer and L. I. Glebova, Inzh.-Fiz. Zh., 6, No. 4 (1963).
3. V. M. Kostylev, Teplofiz. Vys. Temp., 2, No. 1 (1964).
4. R. M. Christiansen and M. Hollingsworth, Adv. Cryog. Eng., 4, 141 (1960).
5. R. M. Christiansen, M. Hollingsworth, and H. N. Marsh, Adv. Cryog. Eng., 5, 171 (1960).
6. J. D. Verschoor and P. Greebler, Trans. ASME, 74, No. 6 (1952).
7. F. C. Wilson, Refrig. Eng., 65, No. 4 (1957).

#### USE OF A DIAMETRAL BLOWER IN A FLOW-THROUGH LASER WITH A CLOSED GAS-CIRCULATION SYSTEM

R. I. Soloukhin, Yu. A. Yakobi,  
E. I. Vyazovich, and S. P. Vagin

UDC 621.378

The choice of a dimetral blower in a closed laser gasdynamic loop is justified and its operation is investigated.

It is known [1] that the specific energy applied to the active medium of electric-discharge gas lasers is limited by two factors — heating and instability of the gaseous plasma. The main method for overcoming them in application to continuously operating lasers is the rapid pumping of gas through the discharge in a time less than the relaxation time of the internal degrees of freedom and the time of development of instabilities [2]. The stability of the discharge essentially depends on the uniformity of the stream. In [3], e.g., upon a decrease in the velocity scatter from 10 to 3% the maximum energy applied in the stable mode grew more than twofold. The reason for this phenomenon is that nonuniformity of the stream leads to superheating of those of its parts which move with a lower velocity. This leads to transverse stratification of the discharge [4]. The zones with increased current density arising in this case are most dangerous from the point of view of contraction of the discharge [5] and considerably reduce the attainable threshold for the total energy input. Local superheats also lead to optical nonuniformity of the medium associated with density gradients. Optical nonuniformities cause radiation losses to scattering in the active medium, as well

---

Institute of Theoretical and Applied Mechanics, Siberian Branch of the Academy of Sciences of the USSR, Novosibirsk. A. V. Lykov Institute of Heat and Mass Exchange, Academy of Sciences of the Belorussian SSR, Minsk. Translated from Inzhenerno-Fizicheski Zhurnal, Vol. 36, No. 1, pp. 62-68, January, 1979. Original article submitted June 6, 1978.